

A Cell-free System for Regulated Exocytosis in PC12 Cells

Julia Avery,* Darren J. Ellis,[†] Thorsten Lang,* Phillip Holroyd,* Dietmar Riedel,* Robert M. Henderson,[‡] J. Michael Edwardson,[‡] and Reinhard Jahn*

*Department of Neurobiology, Max-Planck-Institute for Biophysical Chemistry, Am Fassberg, D-37077 Göttingen, Germany; and [†]Department of Pharmacology, University of Cambridge, Tennis Court Road, Cambridge CB2 1QJ, United Kingdom

Abstract. We have developed a cell-free system for regulated exocytosis in the PC12 neuroendocrine cell line. Secretory vesicles were preloaded with acridine orange in intact cells, and the cells were sonicated to produce flat, carrier-supported plasma membrane patches with attached vesicles. Exocytosis resulted in the release of acridine orange which was visible as a disappearance of labeled vesicles and, under optimal conditions, produced light flashes by fluorescence dequenching. Exocytosis in vitro requires cytosol and Ca²⁺ at concentrations in the micromolar range, and is sensitive to Tetanus toxin. Imaging of membrane patches at diffraction-limited resolution revealed that 42% of docked gran-

ules were released in a Ca²⁺-dependent manner during 1 min of stimulation. Electron microscopy of membrane patches confirmed the presence of dense-core vesicles. Imaging of membrane patches by atomic force microscopy revealed the presence of numerous particles attached to the membrane patches which decreased in number upon stimulation. Thus, exocytotic membrane fusion of single vesicles can be monitored with high temporal and spatial resolution, while providing access to the site of exocytosis for biochemical and molecular tools.

Key words: video microscopy • AFM • membrane fusion • in vitro • exocytosis

Introduction

Neurons release their transmitters by Ca²⁺-triggered exocytosis of synaptic vesicles. Detailed studies of exocytosis in neurons and neuroendocrine cells have revealed that the fusion of the vesicles with the plasma membrane is preceded by a series of maturation steps that the secretory apparatus needs to undergo before acquiring competence for exocytosis (Martin, 1997). In recent years, numerous proteins have been identified that are involved in the regulation and execution of exocytosis. These include highly conserved protein families required for all eukaryotic fusion events such as the SNAP receptors (SNAREs)¹, SM proteins (acronym for sec1/munc18-related proteins), and Rab proteins, as well as numerous additional proteins that may be specialized for neuronal exocytosis (for review, see Jahn and Südhof, 1999). Interactions between these proteins are reversible, and are often associated with conformational changes that probably represent elementary re-

actions in the pathway leading from vesicle docking to membrane fusion. However, it remains a challenge to integrate these reactions into a coherent sequence of events that explains vesicle maturation and priming, Ca²⁺-triggering, and membrane fusion. Whereas some basic understanding of fusion has been achieved (for review, see Jahn and Südhof, 1999), the role of the proteins mediating the preceding steps is still obscure, and because of their sheer complexity the participating reactions remain largely elusive.

A major obstacle to further progress is the limited availability of assays that allow for the reconstitution of vesicle docking and fusion under cell-free conditions. Unlike intracellular fusion events, for which in vitro assays are readily available (Balch et al., 1984; for review, see Rothman, 1994), biochemical studies of regulated exocytosis are largely limited to permeabilized cell preparations which retain a high level of complexity. These assays were instrumental in the identification of cytosolic proteins that are required for exocytosis (Hay and Martin, 1993; Linial and Parnas, 1996; Ann et al., 1997; reviewed in Avery et al., 1999). However, the temporal and spatial resolution of these assays is inherently limited. Furthermore, using this approach it is difficult to

Address correspondence to Reinhard Jahn, Department of Neurobiology, Max-Planck-Institute for Biophysical Chemistry, Am Fassberg, D-37077 Göttingen, Germany. Tel.: 49-551-201-1634. Fax: 49-551-201-1639. E-mail: rjahn@gwdg.de

¹Abbreviations used in this paper: AFM, atomic force microscopy; SNARE, SNAP receptor.

distinguish between those components that are essential for exocytosis and those that have regulatory roles, or are involved in earlier steps in the secretory process such as cytoskeletal rearrangements or secretory vesicle transport.

Cell-free preparations for exocytosis involving isolated vesicles and plasma membranes have previously been described only for few specialized systems, including the sea urchin egg (Vacquier, 1975; Baker and Whitaker, 1978; Crabb and Jackson, 1985) and the exocrine pancreas (MacLean and Edwardson, 1992). Recently, Martin and Kowalchuk (1997) have characterized a membrane fraction derived from PC12 cells that is enriched in plasma membranes with attached secretory vesicles. The authors showed that these vesicles can be induced to release their content under appropriate conditions, suggesting that the preparation retained its competence for exocytosis during isolation. We now describe a novel *in vitro* assay for regulated exocytosis in PC12 cells that has a high temporal and spatial resolution. Sonication of PC12 cells grown on coated coverslips results in the generation of flat, inside-out membrane patches that remain attached to the coverslip and that contain docked secretory vesicles. Ca^{2+} causes the exocytotic fusion of these vesicles which can be monitored by video fluorescence microscopy at the single vesicle level.

Materials and Methods

Cell Culture and Preparation

PC12 cells were grown on 10-cm-diam dishes in RPMI medium supplemented with 10% horse serum, 5% fetal calf serum, 4 mM glutamine, and 60 units/ml each of penicillin and streptomycin. Cells were incubated at 37°C in 10% carbon dioxide and the medium was changed every other day. For the *in vitro* assay, cells were plated onto glass coverslips that had been precoated with a solution of 0.1 mg/ml poly-L-lysine (Sigma) and then incubated overnight in RPMI complete medium.

Preparation of Cell Fragments

PC12 cells grown on coverslips were preincubated for varying amounts of time (5 min to 2 h) in medium supplemented with 10 μM acridine orange. Cells were then sheared by sonication in ice-cold KGlu buffer (20 mM Hepes, pH 7.2, 120 mM potassium glutamate, 20 mM potassium acetate, 2 mM EGTA) containing 2 mM MgATP and 0.5 mM dithiothreitol. Once prepared, the membrane patches remaining attached to the coverslips were immediately transferred to the same buffer containing 5 mg/ml brain cytosol, prepared according to Martin (1989), ready for use in the *in vitro* exocytosis assay.

Electron Microscopy

Coverslips were coated with EM bed 812 (Electron Microscopy Sciences), polymerized for 8 h at 80°C, and then treated with poly-L-lysine. Cells were grown and membrane patches were prepared by sonication as described above. The patches were fixed in 2.5% glutaraldehyde (Electron Microscopy Sciences) for 2 h at room temperature, washed in 0.1 M cacodylate buffer pH 7.4, postfixed with 1% OsO_4 in cacodylate buffer, followed by a wash with distilled H_2O , and then treated with 1% uranyl acetate. The samples were then dehydrated in ethanol and embedded in EM bed 812. After polymerization at 60°C for 48 h the coverslips were removed by etching with hydrofluoric acid. Ultrathin sections were cut perpendicular to the monolayer and stained with uranyl acetate and lead citrate.

Monitoring of Membrane Fusion by Fluorescence Video Microscopy

Membrane patches were analyzed using a Zeiss Axiophot 2 fluorescence

microscope with a 100 \times 1.4 NA plan achromate. Once a particular field was in focus, the solution was changed by capillary action and replaced with KGlu buffer containing 2 mM MgATP, 0.5 mM dithiothreitol, and, where appropriate, various concentrations of free Ca^{2+} and cytosol (0.5 mg/ml protein). Ca^{2+} was buffered with 2 mM EGTA, and free Ca^{2+} concentrations were calculated as described by Föhr et al. (1993). For imaging, we used either a video-intensified CCD camera or a slow-scan CCD camera (both from Princeton Instruments Inc.). Images were processed using Metamorph 3.5 (Universal Imaging Corp.). Both acridine orange dequenching and FM1-43 labeling were detected using Zeiss filter set 10 (excitation filter BP 450-490, BS 510, emission filter BP 515-565), except the results shown in Figs. 3–5 for which Zeiss filter set 09 (excitation filter BP 450-490, BS 510, emission filter LP 520) was used.

For pretreatment of the patches with Tetanus toxin, cells were sonicated and incubated for 10 min at 37°C in KGlu buffer containing 1.7 μM acridine orange and 8 μM Tetanus toxin light chain as indicated. The coverslips were then mounted on the microscope and an area containing between one and five patches was imaged. The solution was changed by capillary action and replaced with KGlu buffer containing 0.5 mg/ml rat brain cytosol and, where indicated, 100 μM free Ca^{2+} . At the times indicated pictures of the selected area were taken. Images were high-pass filtered with a spatial frequency of 1/500 nm. Changes in the number of spots after buffer exchange were quantitated by counting.

Atomic Force Microscopy (AFM) Imaging

AFM imaging was performed using a BioScope Atomic Force Microscope (Digital Instruments). PC12 cell plasma membrane patches were prepared for AFM by *in situ* fixation with 4% paraformaldehyde followed by rinsing with ultrapure water to prevent salt crystallization and air-drying. Commercially available, 125- μm -long Si_3N_4 cantilevers oscillating at \sim 5% resonance frequency (typically \sim 320 kHz) with a root mean squared amplitude of 0.7 V were used (Nanosensors GmbH). Images were captured using tapping-mode AFM after feedback gains and scan speed (typically $<$ 1.5 Hz) had been optimized.

AFM of native (i.e., unfixed and wet) membrane patches was achieved using the BioScope's fluid cell and commercially available, oxide-sharpened Si_3N_4 cantilevers (Nanoprobes; Digital Instruments) with a force constant of \sim 0.34 N/m. Freshly prepared fragments on coverslips were stably settled in shallow 35-mm tissue culture dishes on a small bed of high vacuum grease (Dow Corning); this prevented movement of the coverslip during imaging. Tissue culture dishes were filled with potassium glutamate buffer containing 1 mg/ml rat brain cytosol to a depth of 3–4 mm before transfer to the atomic force microscope. Samples were initially engaged in contact mode with the scan size set to zero to prevent sample damage. A force curve was captured to provide primary verification of cantilever integrity. The tip was then raised 50 μm above the surface, and any air bubbles present near the fluid cell were removed. The microscope was set to tapping mode with a root mean squared amplitude of \sim 0.7 V and a drive frequency of 8–9 kHz before re-engagement. Membrane patches were identified. While the tip was still engaged, enough 1 M CaCl_2 was gently added to the imaging buffer to give a final concentration of 10 μM , and successive images were captured.

Results

Cell-free Exocytosis of Secretory Vesicles on Patches of Plasma Membrane Monitored after Labeling with Acridine Orange

To generate carrier-supported plasma membranes with attached secretory vesicles, PC12 cells were grown to near confluence on polylysine-coated coverslips and sonicated. Analysis by phase contrast microscopy revealed that in addition to intact cells, many footprint-like flat structures were visible that were devoid of nuclei. In an initial characterization, the slides were fixed and processed for immunocytochemistry. Staining for the vesicle proteins synaptobrevin, synaptotagmin, and synaptophysin resulted in strong and punctate labeling, whereas staining for SNAP-25 showed a widespread distribution over the membrane

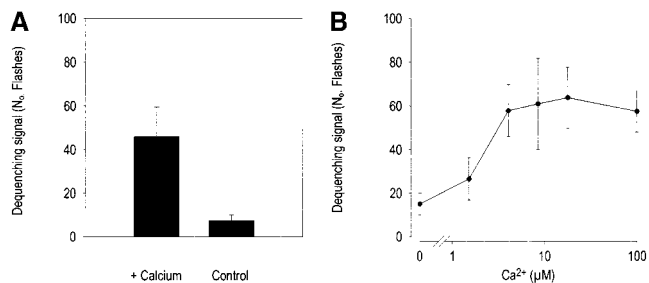


Figure 1. Exocytosis of secretory vesicles from membrane patches, monitored by fluorescence dequenching of acridine orange. Cortical fragments prepared from PC12 cells prelabeled with acridine orange were analyzed by fluorescence microscopy. (A) Quantitation of the dequenching signals (by manual counting) in the field of view for fragments perfused with either 10 μM Ca^{2+} or with control buffer containing 2 mM EGTA. Values are means \pm SEM; $n = 7$, plus Ca^{2+} and $n = 3$, control. (B) Ca^{2+} sensitivity of exocytosis *in vitro*. Half-maximal stimulation occurred at approximately 2 μM Ca^{2+} . Values are means \pm SEM ($n = 3$).

patches (data not shown). In contrast, no fluorescence signals were seen when membrane patches were stained with mitotracker-green FM, which detects mitochondria (not shown, see also below). These observations indicated that the majority of the cell's cytoplasmic structures was removed during the sonication procedure to leave a minimal structure comprising the plasma membrane and attached secretory vesicles.

To monitor exocytosis, PC12 cells were incubated in medium containing acridine orange before sonication. As a result, the dye accumulated inside acidic compartments. In such compartments, acridine orange is known to form dimers or higher aggregates, which causes quenching of its fluorescence at 530 nm (Palmgren, 1991). After sonication, the membrane patches were incubated in buffer containing 2 mM MgATP and 5 mg/ml cytosol and subsequently superfused with potassium glutamate buffer containing either Ca^{2+} (at the concentration indicated) or, as a control, 2 mM EGTA. Upon exocytosis, the dye was discharged into the extracellular space and became rapidly diluted, resulting in a disappearance of the labeled granule. Because

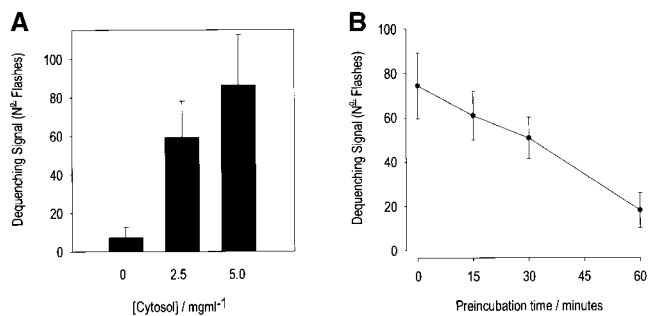


Figure 2. Cytosol dependence of exocytosis *in vitro*, measured as in Fig. 1. (A) Membrane patches were prepared in physiological buffer containing the indicated concentrations of rat brain cytosol, before the addition of 10 μM Ca^{2+} . Values are means \pm SEM ($n = 3$). (B) Membrane patches were incubated at 37°C for the times indicated in the presence of cytosol (5 mg/ml), before the addition of Ca^{2+} . Values are means \pm SEM ($n = 6$).

dilution results in dequenching, exocytotic events caused transient flashes of fluorescent light that were recognizable under the microscope.

In an initial series of experiments we examined whether the dequenching signals exhibit characteristics typical of exocytosis from permeabilized PC12 cells (Martin, 1997). For this purpose, the number of flashes occurring in the field of view in a 3-min period after the addition of Ca^{2+} -containing or control buffer was counted. As shown in Fig. 1, Ca^{2+} caused a substantial increase in the number of dequenching flashes over those occurring in the presence of EGTA alone, indicating that the signals arose as a result of exocytosis. In the absence of Ca^{2+} , occasional light flashes were visible that depended on the light intensity. These signals can probably be attributed to photolysis of the secretory granules (Brunk et al., 1997). The Ca^{2+} sensitivity of the response was also measured by perfusing with a range of Ca^{2+} concentrations. As shown in Fig. 1 B, half-maximal stimulation was obtained at ~ 2 μM Ca^{2+} . This value is similar to that obtained using both permeabilized chromaffin cells (Holz et al., 1989) and PC12 cells (Martin and Kowalchuk, 1997). Furthermore, exocytosis was de-

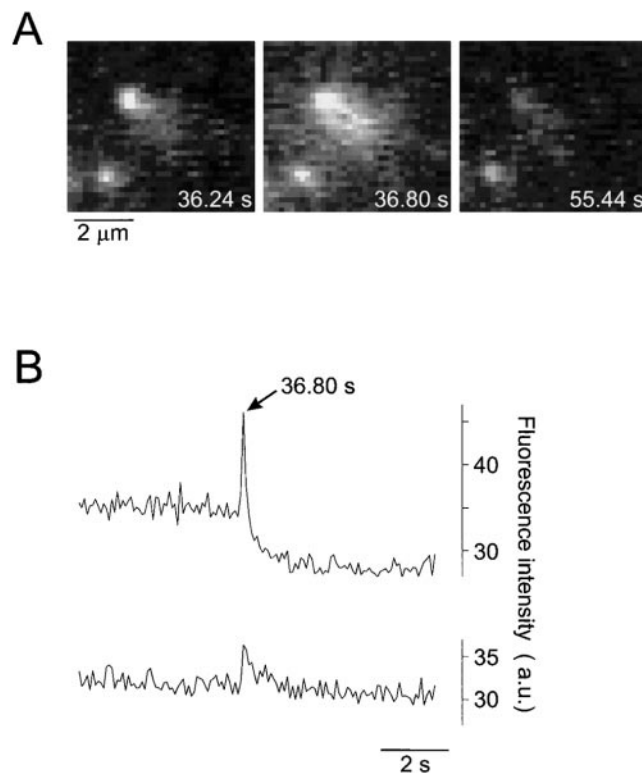


Figure 3. Dequenching flash caused by exocytosis of an acridine-orange-loaded secretory vesicle, imaged by video microscopy at a rate of 25 Hz. (A) Sequence of video images showing a typical dequenching flash arising from a fluorescent spot (left). The delay time after the addition of Ca^{2+} is indicated. Note that after the flash the spot is largely diminished whereas a second spot (lower right) remains unchanged. (B) Fluorescence intensity profile of the dequenching flash shown in the sequence. A circular mask with a diameter of 10 pixels was centered over both spots. The average intensity was determined for every second frame over the sequence and plotted against time. The blip in the intensity profile of the lower spot is caused by a spillover of acridine orange during exocytosis of the upper spot. a.u., arbitrary units.

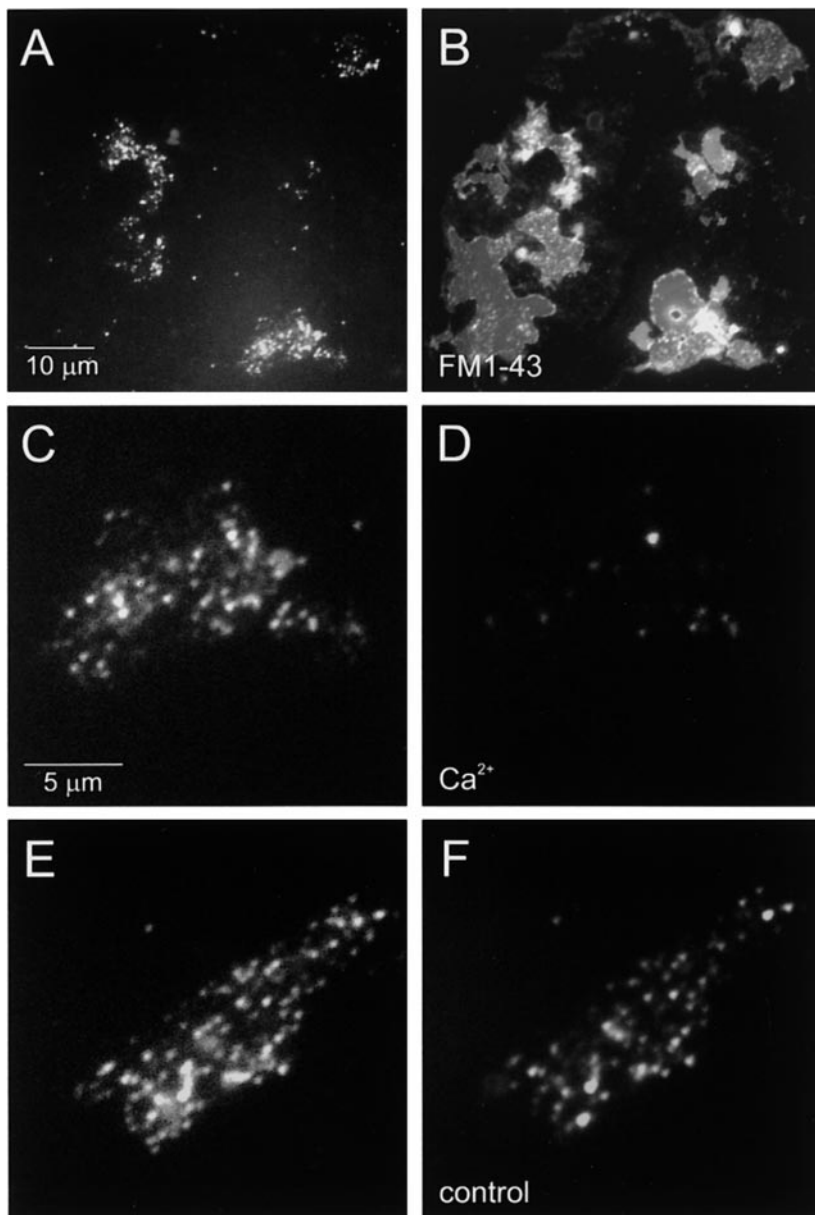


Figure 4. Disappearance of acridine-orange-labeled particles after Ca^{2+} stimulation. Membrane patches were prepared from cells preloaded with acridine orange and imaged in incubation buffer containing rat brain cytosol and ATP. (A) Low magnification of labeled membrane patches. (B) Same field as in A but labeled at the end of the experiment with FM1-43 in order to visualize all phospholipid membranes. (C–F) High magnification of membrane patches before (C and E) or after a 1-min treatment with $100 \mu\text{M Ca}^{2+}$ (D) or control buffer (F).

pendent on the presence of cytosol (Fig. 2 A). Extending the preincubation time resulted in a gradual rundown of the exocytotic signals despite the continued presence of cytosol and ATP (Fig. 2 B). Together, these findings are in good agreement with previous reports on exocytosis in permeabilized PC12 cells (reviewed by Martin, 1997; Avery et al., 1999).

For further analysis, the acridine orange signals were monitored with an intensified video camera using a frame rate of 25 Hz. Fig. 3 (A) shows images of two granules, one of which is undergoing exocytosis, before, during, and after the light flash. During the flash, the fluorescence intensity rose sharply and then decreased within a few hundred milliseconds (Fig. 3 B).

Using a slow-scan CCD camera, we also recorded at diffraction-limited resolution the distribution of dye-containing organelles on the membrane patches before and

after a 1-min stimulus with $100 \mu\text{M Ca}^{2+}$ (Fig. 4). Before stimulation, the patches were incubated for 2 min with 10-fold concentrated cytosol and ATP in the absence of Ca^{2+} (see Materials and Methods) to fully prime the vesicles. Under control conditions, numerous fluorescent spots were visible (Fig. 4, A, C, and E). Superfusion with Ca^{2+} -containing buffer led to a reduction in the number of spots (compare Fig. 4, C and D) which was not observed when EGTA was used instead (Fig. 4, E and F). To assess this effect more precisely, the disappearance of spots was quantitated in a series of membrane patches. The reduction was $58.5\% \pm 5.6\%$ upon stimulation with $100 \mu\text{M Ca}^{2+}$ ($n = 17$) and $16.4\% \pm 5.4\%$ for control (unstimulated) patches incubated in parallel ($n = 12$). To confirm that the disappearance of granules is due to exocytosis, patches were pretreated for 10 min with Tetanus toxin light chain before the addition of cytosol, ATP and Ca^{2+} .

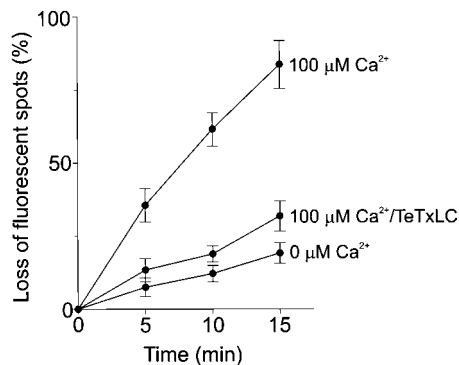


Figure 5. Ca²⁺-dependent disappearance of labeled particles is blocked by preincubation of the patches with Tetanus toxin light chain. At the times indicated, the patches were imaged and the loss of particles was determined by counting. Note that in this experiment, ATP was added together with Ca²⁺ and cytosol, and the cytosol concentration was lower than that in the experiment shown in Fig. 4, resulting in a slower time course of exocytosis. Each data point represents the mean value of 15–20 patches obtained from six independent preparations except the 15 min data points for which 4–8 patches were used.

As expected for exocytosis, toxin pretreatment largely prevented the disappearance of fluorescent dots regardless of whether Ca²⁺ was elevated (Fig. 5). In this experiment, ATP was added together with Ca²⁺ and the preincubation with concentrated cytosol was omitted, resulting in a slower time course of exocytosis than that described above (Fig. 5).

Imaging of Membrane Patches Using Electron Microscopy and AFM

In the following experiments, we used two complementary high-resolution microscopy approaches in order to confirm that the events described above are indeed caused by the exocytosis of dense-core secretory vesicles. First, membrane patches obtained from Ca²⁺- or EGTA-treated samples were fixed and embedded for electron microscopy. An analysis of unstimulated patches revealed the presence of numerous dense-core secretory granules that

were attached to the membrane patch (Fig. 6 A). No other organelles were observed, with the exception of occasional clathrin-coated vesicles. When patches were stimulated with Ca²⁺-containing buffer, the number of secretory granules was significantly decreased (Fig. 6 C).

Second, membrane patches were imaged using AFM. AFM reveals the topography of the membrane patch by mechanically moving a sharp Si₃N₄ probe over the fragment to ‘feel’ the contours of the surface. Unlike other high-resolution, radiation-based microscopic techniques, AFM can be applied to both native and fixed specimens either in air or under physiological buffers. When fixed, nonstimulated membrane patches were imaged, the contours of the membrane patches were clearly visible (Fig. 7, A and B). On these patches, an array of raised structures bound to the plasma membrane was observed which probably represent predominantly secretory granules. In addition, larger structures were occasionally seen that may represent membrane infoldings such as those observed in the electron microscope (see Fig. 6). It was also apparent that the membranes themselves were free from preparation damage, shown by the absence of holes or tears (Fig. 7). Again, these findings agree with the light microscopic images obtained after labeling of the membranes with the dye FM1-43 (Fig. 4 B). Furthermore, acridine orange loading had no detectable effect on the structure of the membrane patches and the appearance of the particles (data not shown).

The majority of the raised structures was relatively uniform in size and shape (Fig. 7, C and D), with a mean height of 34 ± 0.4 nm and a mean full-height diameter of 225 ± 2 nm ($n = 77$). These dimensions probably reflect flattening of the vesicles during drying down of the samples. The diameter of mature secretory vesicles in PC12 cells is ~ 120 nm (Tooze et al., 1991; see also Fig. 6 B). A sphere of this structure has a volume of $905,000$ nm³ ($V = 4/3\pi r^3$). Assuming that the vesicles collapse into an ellipsoid with a height (r_1) of 34 nm and two equal semi-axes (radius r_2), the predicted diameter of the ellipsoid, calculated using the formula $V = 4/3\pi r_1 r_2^2$, would be 225 nm, the value actually observed.

When the patches were treated with Ca²⁺ before fixation, a dramatic reduction in the number of these particles was observed (compare Fig. 8, A and B). Such a reduction

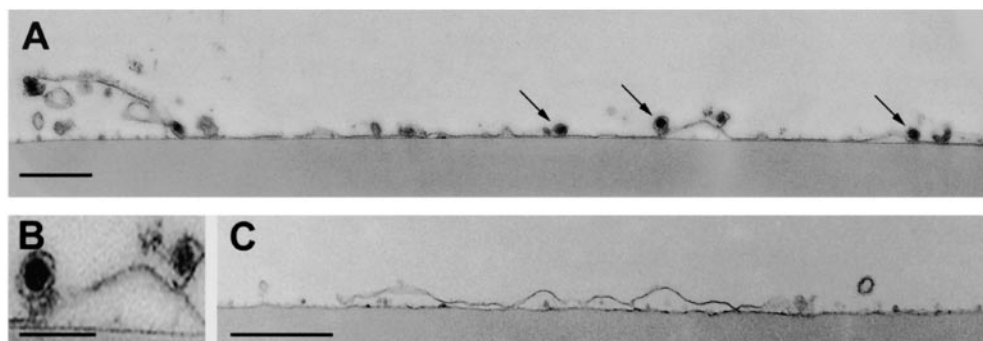


Figure 6. Cross-sections of membrane patches analyzed by electron microscopy. The fragments were incubated either in the presence of 2 mM EGTA (A) or in the presence of 100 μM Ca²⁺ (C) for 3 min before fixation. Several secretory vesicles (arrowheads) are attached to the cytoplasmic face of the plasma membrane in the EGTA-treated patch. (B) Two secretory vesicles at higher magnification. Bars: (A and C) 0.5 μm; (B) 0.25 μm.

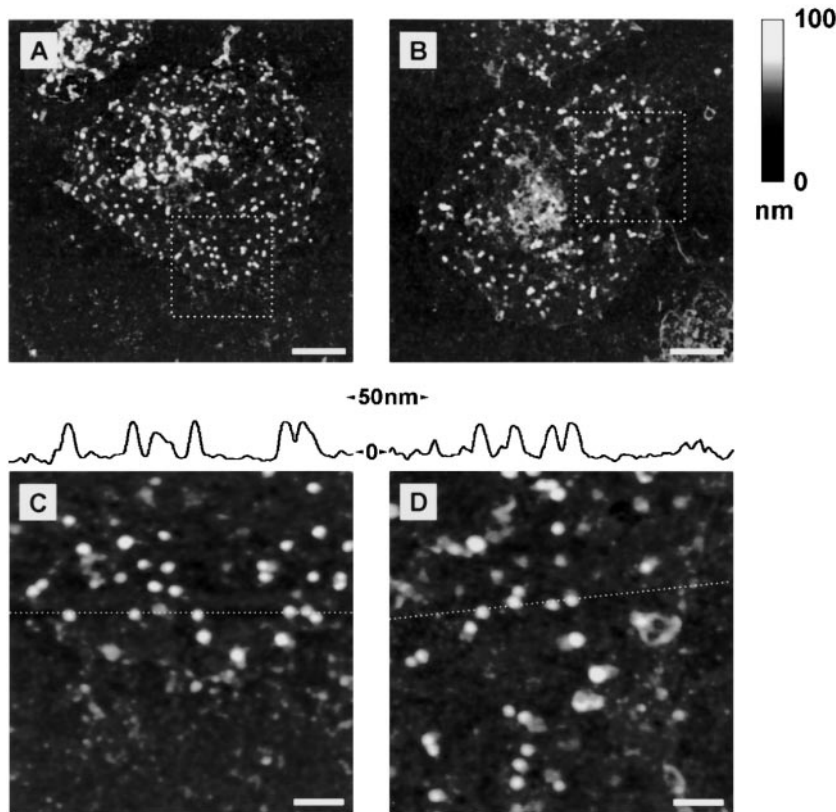


Figure 7. AFM imaging of membrane patches, imaged in air using tapping mode. A and B show two membrane patches representative of those used in the *in vitro* assay for exocytosis. Boxed areas in A and B are magnified in C and D, respectively. C and D show individual particles. Dotted lines denote the line of cross-section shown above C and D. The mean particle height was 34 ± 0.4 nm and the mean diameter was 225 ± 2 nm (means \pm SEM, $n = 77$). AFM images are black/white-coded with respect to height; a height scale is shown on the right. Bars: (A and B) $2 \mu\text{m}$; (C and D) 500 nm.

was consistently observed in several independent experiments even though the density of the particles differed between individual preparations (see Discussion). These observations agree well with those described above using acridine orange labeling (see Fig. 4).

Finally, we performed repetitive scans of unfixed membrane patches under fluid while they were stimulated in order to monitor the fusion of secretory vesicles. Five successive images were captured over a total time of ~ 22 min during which Ca^{2+} was raised to $10 \mu\text{M}$. Fig. 9 shows that a cluster of raised structures disappeared between the second and the third scan without any change in the overall profile of the membrane patches. After the disappearance of the raised particles, the patch remained stable. Interestingly, we occasionally observed the appearance of raised particles after stimulation that may represent the generation of endocytic vesicles (not shown) but more experiments are needed to assess the significance of these observations.

To confirm that the disappearance of the particles was a result of exocytotic membrane fusion, similar experiments were performed in the absence of either Ca^{2+} or cytosol. Under these conditions, no disappearance of particles was seen (data not shown) indicating that the scanning probe does not sweep secretory granules off the membrane and does not damage the structure of the membrane itself. Although this procedure is not suitable for routine applications due to the unavoidably slow setup and recording times, the data support our view that Ca^{2+} -dependent exocytosis occurs on patches. Note that the resolution of un-

fixed membrane patches is lower than that of fixed, dry patches. This is probably due to the presence of cytosol-containing buffer of high viscosity which might degrade the performance of the microscope in tapping mode.

Discussion

In this study, we describe a cell-free assay for regulated exocytosis in PC12 cells which allows a study of the membrane fusion of single secretory vesicles at high spatial and temporal resolution. Exocytosis is dependent on ATP, cytosol, and Ca^{2+} , and thus resembles exocytosis in permeabilized cells (Martin, 1997).

Our assay takes advantage of the fact that the weak base acridine orange accumulates within acidic compartments, which under our conditions are predominantly secretory vesicles. This feature has previously been used to label secretory vesicles in experiments with intact chromaffin cells involving total internal reflection microscopy (Steyer et al., 1997). In these experiments, acridine orange-loaded secretory granules were imaged as fluorescent spots selectively in the subplasmalemmal area of the cell (i.e., the site where the cell is attached to the glass coverslip). Upon stimulation, spots disappeared. Furthermore, loss of spots correlated with the detection of amperometric spikes suggesting that the loss is due to exocytotic release of acridine orange. The assay described here is similar except that most of the cytoplasm is removed and the release sites are exposed to the medium, a prerequisite for biochemical

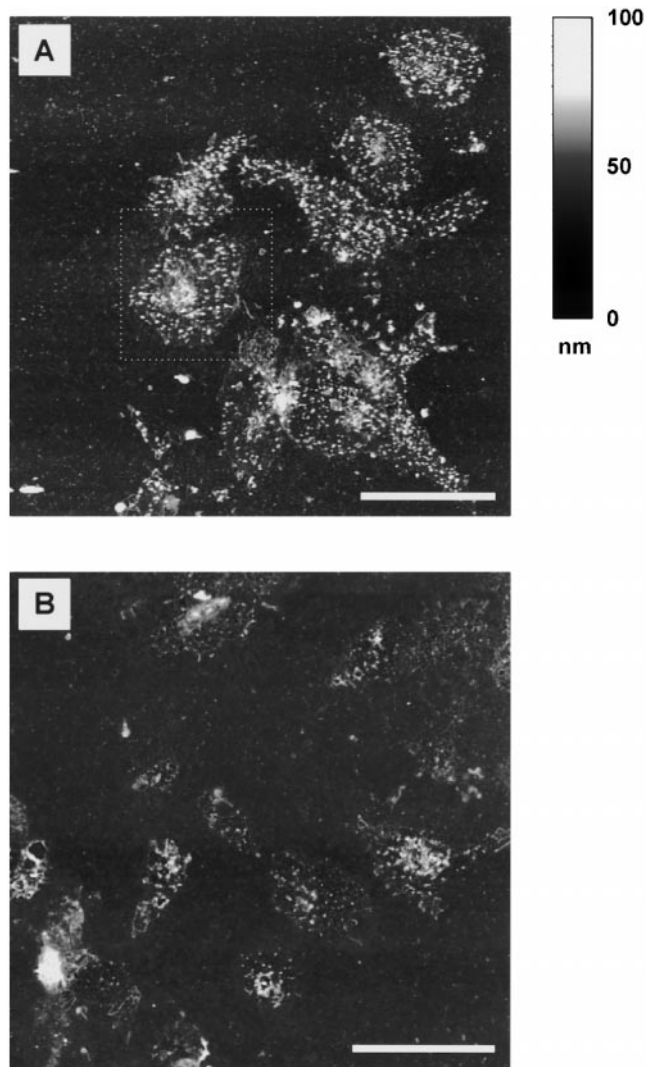


Figure 8. Incubation in Ca^{2+} -containing buffer causes disappearance of particles as expected for exocytosis. Freshly prepared membrane patches were incubated for 5 min in medium supplemented with either 2 mM EGTA (A) or 10 μM Ca^{2+} (B) and then fixed as described in Materials and Methods. Fixed samples were imaged in air using tapping-mode AFM. These low-magnification images show two fields each containing ~ 10 membrane patches. The boxed area is the same as that shown at higher magnification in Fig. 6 B. The membrane patches in A contain numerous particles on their surfaces. Following incubation in 10 μM Ca^{2+} (B) the membrane patches have fewer particles, consistent with the disappearance of secretory vesicles due to Ca^{2+} -triggered exocytosis. Bars, 10 μm .

manipulations. In PC12 cells, many of the large, dense-core vesicles containing catecholamines are docked at the plasma membrane (Schäfer et al., 1987), a further advantage of this model system.

Acridine orange will label not only secretory vesicles but also other acidic compartments, such as endosomes and lysosomes. However, in our electron microscopic analysis secretory granules were the predominant organelles bound to the plasma membrane, suggesting that

each acridine-orange-positive spot represents an individual secretory vesicle, and also that each light flash is caused by the release of dye from a single vesicle. It should be borne in mind that dye release may also be caused by light-induced photolysis of granules (Brunk et al., 1997). Indeed, we observed that the frequency of flashes increased in parallel with the light intensity. This increase, however, was independent of the presence of Ca^{2+} , cytosol, or ATP, thus allowing us to distinguish photolysis from true exocytotic events. That exocytosis did indeed occur upon Ca^{2+} stimulation was confirmed by the concomitant disappearance of vesicles observed both by electron microscopy and by AFM. The assay should be easily adaptable to alternative means of labeling, for instance in the study of cells transfected with GFP-tagged proteins that are targeted to secretory granules (Lang et al., 1997; Kaether et al., 1997).

Some variability was observed with respect to the number of vesicles attached to each membrane patch. This can be attributed to one of several factors. First, the pulse frequency, intensity, and duration of the ultrasonic pulse are critical, in that an optimum needs to be found between inefficient disruption of the cells and blasting away of the granules. That the latter can occur was observed in experiments using higher energy settings (unpublished observations). In these experiments, patches of plasma membrane were still attached to the coverslip but they were devoid of granules. Second, PC12 cell lines obtained from different sources appear to vary with respect to the amount of docked vesicles. Furthermore, they appear to undergo drifting towards lower number of vesicles upon increasing passage numbers. During the course of the last three years we have switched several times to new batches of PC12 cells, and have observed changes in the density of docked vesicles. Acridine orange labeling, however, allows for a visualization of all vesicles at the beginning and end of each experiment, provided that an appropriate filter set and a high-resolution video camera are available. With this method (Fig. 4) we were able to relate exocytosis to the total pool of granules docked at the beginning of each experiment. Since it is fast and easy to perform, we now use it for routine applications as the method of choice.

The extent to which the vesicles attached to the plasma membrane is committed to exocytosis, and how far they have progressed in the pathway towards membrane fusion both remains to be established. Preliminary results indicate that incubation with cytosol and ATP for several minutes does not lead to a significant degree of undocking, although the cause of the slight but significant loss of vesicles under these conditions needs to be explained. On the other hand, the vesicles attached to the membrane require priming, since Ca^{2+} alone in the absence of cytosol and ATP inefficiently triggers to elicit exocytosis. Thus it is unlikely that the docked vesicles have progressed far towards fusion, for instance, by forming trans-SNARE complexes. Given that our assay can easily be adapted to laminar superfusion with precisely timed solution changes on a millisecond time scale, it should be possible to determine the sequential requirements for these factors and, furthermore, to elucidate whether readily releasable vesicle pools can be distinguished, such as those recently described for adrenal chromaffin cells (Neher, 1998).

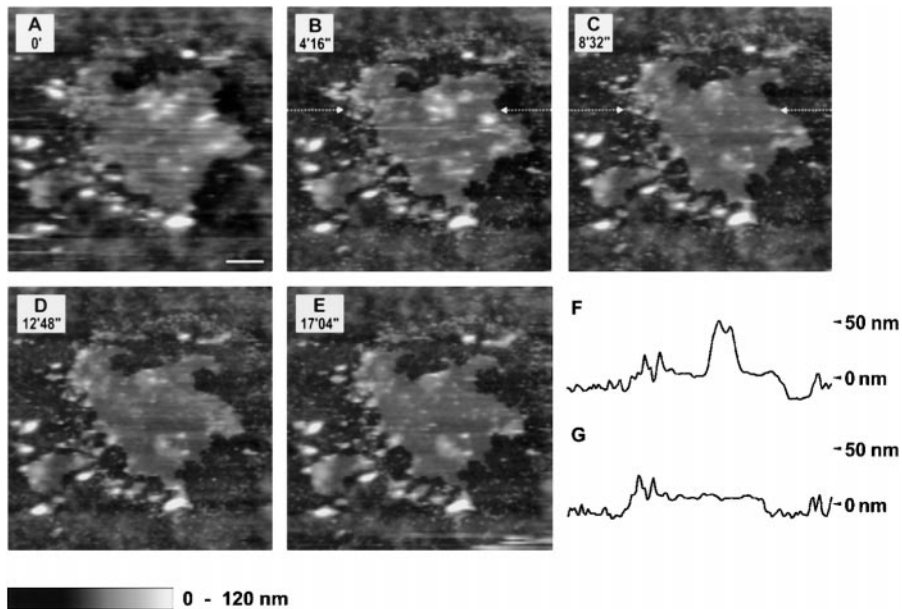


Figure 9. Live AFM imaging of Ca^{2+} -triggered exocytosis. Freshly prepared and unfixed membrane patches were identified by AFM. After the capture of the image shown in A and while the tip was still engaged, Ca^{2+} (final concentration $10 \mu\text{M}$) was gently added at time zero to the imaging buffer. To avoid disrupting the probe, the Ca^{2+} was added very gently at the edge of the sample and the solution stirred very gently by pipetting up and down. This was to avoid disengaging the probe from the surface. The time delay between Ca^{2+} addition and exocytosis therefore probably represents the time taken for the diffusing calcium to reach a sufficiently high (threshold) level to trigger exocytosis. The membrane patch in this series of images is visible as a plateau of uniform grey. Taller particles are seen as lighter regions. Between time points B and C a cluster of particles (indicated by the arrows) dis-

appears in response to Ca^{2+} . The dotted lines in B and C denote the line of the cross-sectional height profile shown in F and G, respectively. During the remainder of the time-course neither the shape of the membrane patch nor other surface features are disrupted by repeated scanning. This series of images is representative of the results of 4 experiments. Bar, $2 \mu\text{m}$.

The authors wish to thank all members of the Jahn lab for helpful discussions.

This research was supported by a project grant from the Biotechnology and Biological Sciences Research Council (to R.M. Henderson and J.M. Edwardson).

Submitted: 19 July 1999

Revised: 10 December 1999

Accepted: 10 December 1999

References

- Ann, K., J.A. Kowalchuk, K.M. Loyet, and T.F.J. Martin. 1997. Novel Ca^{2+} -binding protein (CAPS) related to UNC-31 required for Ca^{2+} -activated exocytosis. *J. Biol. Chem.* 272:19637-19640.
- Avery, J., R. Jahn, and J.M. Edwardson. 1999. Reconstitution of regulated exocytosis in cell-free systems: a critical appraisal. *Annu. Rev. Physiol.* 61:777-807.
- Baker, P.F., and M.J. Whitaker. 1978. Influence of ATP and calcium on the cortical reaction in sea urchin eggs. *Nature.* 276:513-515.
- Balch, W.E., B.S. Glick, and J.E. Rothman. 1984. Sequential intermediates in the pathway of intercompartmental transport in a cell-free system. *Cell.* 39:525-536.
- Brunk, U.T., H. Dalen, K. Roberg, and H.B. Hellequist. 1997. Photo-oxidative disruption of lysosomal membranes causes apoptosis of cultured human fibroblasts. *Free Radic. Biol. Med.* 23:616-626.
- Crabb, J.H., and R.C. Jackson. 1985. In vitro reconstitution of exocytosis from plasma membrane and isolated secretory vesicles. *J. Cell Biol.* 101:2263-2273.
- Föhr, K.J., W. Warchol, and M. Gratzl. 1993. Calculation and control of free divalent cations in solutions used for membrane fusion studies. *Methods Enzymol.* 221:149-157.
- Hay, J.C., and T.F.J. Martin. 1993. Phosphatidylinositol transfer protein required for ATP-dependent priming of Ca^{2+} -activated secretion. *Nature.* 366:572-575.
- Holz, R.A., M.A. Bittner, S.C. Peppers, R.A. Senter, and D.A. Eberhard. 1989. MgATP-independent and MgATP-dependent exocytosis. *J. Biol. Chem.* 264:5412-5419.
- Jahn, R., and T.C. Südhof. 1999. Membrane fusion and exocytosis. *Annu. Rev. Biochem.* 68:863-911.
- Kaether, C., T. Salm, M. Glombik, W. Almers, and H.H. Gerdes. 1997. Targeting of green fluorescent protein to neuroendocrine secretory granules: a new tool for real time studies of regulated protein secretion. *Eur. J. Cell Biol.* 74:133-142.
- Lang, T., I. Wacker, J. Steyer, C. Kaether, I. Wunderlich, T. Soldati, H.H. Gerdes, and W. Almers. 1997. Ca^{2+} -triggered peptide secretion in single cells imaged with green fluorescent protein and evanescent-wave microscopy. *Neuron.* 18:857-863.
- Linial, M., and D. Parnas. 1996. Deciphering neuronal secretion: tools of the trade. *Biochim. Biophys. Acta.* 1286:117-152.
- MacLean, C.M., and J.M. Edwardson. 1992. Fusion between rat pancreatic zymogen granules and pancreatic plasma membranes. Modulation by a GTP-binding protein. *Biochem. J.* 286:747-753.
- Martin, T.F.J. 1989. Cell cracking: permeabilizing cells to macromolecular probes. *Methods Enzymol.* 168:225-233.
- Martin, T.F.J. 1997. Stages of regulated exocytosis. *Trends Cell Biol.* 7:271-276.
- Martin, T.F.J., and J.A. Kowalchuk. 1997. Docked secretory vesicles undergo Ca^{2+} -activated exocytosis in a cell-free system. *J. Biol. Chem.* 272:14447-14453.
- Neher, E. 1998. Vesicle pools and Ca^{2+} microdomains: new tools for understanding their roles in neurotransmitter release. *Neuron.* 20:389-399.
- Palmgren, M.G. 1991. Acridine orange as a probe for measuring pH gradients across membranes: mechanism and limitations. *Anal. Biochem.* 192:316-321.
- Rothman, J.E. 1994. Mechanisms of intracellular protein transport. *Nature.* 372:55-63.
- Schäfer, T., U.O. Karli, E.K.-M. Gratwohl, F.E. Schweizer, and M.M. Burger. 1987. Digitonin-permeabilized cells are exocytosis competent. *J. Neurochem.* 49:1697-1707.
- Steyer, J.A., H. Horstmann, and W. Almers. 1997. Transport, docking and exocytosis of single secretory granules in live chromaffin cells. *Nature.* 388:474-478.
- Tooze, S.A., T. Flatmark, J. Tooze, and W.B. Huttner. 1991. Characterization of the immature secretory granule, an intermediate in granule biogenesis. *J. Cell Biol.* 115:1491-1503.
- Vacquier, V. 1975. The isolation of intact cortical granules from sea urchin eggs: calcium ions trigger granule discharge. *Dev. Biol.* 43:62-74.